

Effect of Heat Source and Thermal-Diffusion on MHD Heat and Mass Transfer Flow of a Micropolar Fluid over a Vertical Permeable Plate

B. I Olajuwon¹, J.I. Oahimire²

¹Department of Mathematics, Federal University of Agriculture, Abeokuta, Nigeria.

²Department of Mathematics, University of Port Harcourt, Port Harcourt, Nigeria.

Abstract

This study presents a mathematical analysis of heat and mass transfer effects on unsteady flow of a micropolar fluid over an infinite moving permeable plate in a saturated porous medium in the presence of a transverse magnetic field. The governing system of partial differential equations is transformed to dimensionless equations using dimensionless variables. The resulting dimensionless equations are then solved analytically using perturbation technique to obtain the expression for velocity, microrotation, temperature and concentration. With the help of graphs, the effects of the various important parameters entering into the problem on the velocity, microrotation, temperature and concentration fields within the boundary layer are discussed. Also the effects of the pertinent parameters on the skin friction coefficient, couple stress coefficient and the rate of heat and mass transfer in terms of the Nusselt number and Sherwood numbers are discussed. The results show that the observed parameters have significant influence on the flow, heat and mass transfer.

Keywords: Micropolar fluid, perturbation technique, heat and mass transfer, heat source and thermal-diffusion.

Nomenclatures

B_0 , magnetic field strength; stress;	n_1 , parameter related to microgyration vector and shear stress;
C , mass concentration ;	K' , permeability parameter;
C_f , skin friction coefficient;	Nu , Nusselt number
C_w , couple stress coefficient;	n , scale constant;
C_p , specific heat at constant pressure;	Pr , Prandtl number;
D , chemical molecular diffusivity;	Sc , Schmidt number;
g , acceleration due to gravity ;	Sh , Sherwood number;
V_0 , scale of suction velocity ;	t , time;
Gc , modified Grashof number;	T , temperature;
Gr , Grashof number;	u, v , components of velocities;
j , microinertia per unit mass;	U_0 , scale of free stream velocity;
K , permeability of the porous medium;	x, y distance along and perpendicular to the plate;
M , magnetic field parameter;	Sr , Soret number;
U_p , velocity of the plate;	Q_0 , constant heat flux per unit;
T_m , mean temperature of the fluid;	
K_t , thermal diffusion ratio;	
Greek symbol	
α , fluid thermal diffusivity;	μ , fluid dynamic viscosity;
β , ratio of vortex viscosity and dynamic viscosity;	ρ , fluid density;
β_c , coefficient of volumetric mass expansion ;	σ , electrical conductivity;
β_T , coefficient of volumetric thermal expansion ;	ν , fluid kinematic viscosity;
γ , spin gradient viscosity;	ν_r , fluid kinematic rotational viscosity;
w , angular velocity vector;	θ , dimensionless temperature;
ε , scalar constant ($\ll 1$);	
λ , coefficient of vortex viscosity;	

Corresponding author: **B. I Olajuwon** E-mail: ishola1@gmail.com, Tel.: +2348033791102, +2348155011926

1.0 Introduction

The general theory of micropolar fluids deviates from that of Newtonian fluids by adding two new variables to the velocity. These variables are microrotations that are spin and microinertia tensors describing the distributions of atoms and molecules inside the microscopic fluid particles. Micropolar fluids are those consisting of randomly oriented particles suspended in a viscous medium, which can undergo a rotation that can affect the hydrodynamics of the flow, making it distinctly non-Newtonian fluid. The theory of Micropolar fluids originally developed by Eringen [1] has been a popular field of research in recent years. This theory takes into account the effect of local rotary inertia and couple stresses arising from practical microrotation action. It is applied to suspensions, liquid crystals, polymeric fluids and turbulence. This behavior is familiar in many engineering and physical applications.

If two regions in a mixture are maintained at different temperatures so that there is a flux of heat, it has been found that a temperature gradient is set up. In a binary mixture, one kind of a molecule tends to travel toward the hot region and the other kind toward the cold region. This is called the 'Soret effect'. When the flow of mass is caused by a temperature difference one cannot neglect the thermal diffusion effect (commonly known as Soret effect) due to its practical application in engineering and science. Usually this effect has a negligible influence on mass transfer, but it is useful in the separation of certain mixtures. Thermal diffusion effect or Soret effect has been utilized for isotope separation in mixtures between gases with very light molecular weight (H_2 , He) and medium molecular weight (N_2 , air) and it was found to be of a magnitude that it cannot be neglected.

The study of heat generation or absorption effects in moving fluids is important in view of several physical problems, such as fluid undergoing exothermic or endothermic chemical reaction. Possible heat generation effects may alter the temperature distribution and consequently, the particle deposition rate in nuclear reactors, electric chips and semiconductor wafers. In certain applications such as those involving heat removal from nuclear fuel debris, underground disposal of radioactive waste material, storage of food stuffs, and exothermic chemical reaction and dissociating fluids in packed-bed reactors, the working fluid heat generation or absorption effects are important. Based on these applications, Soret effects due to natural convection between heated inclined plates have been investigated by Raju [2]. Aurangzaib [3] investigated the effects of Soret and Dufour on heat and mass transfer over an unsteady MHD flow by mixed convection over a vertical surface in porous media in the presence of internal heat generation with chemical reaction, hall current and thermal radiation. Kumar and Singh [4] studied Soret and hall effects on oscillatory MHD free convection flow of a radiating fluid in a rotating vertical porous channel filled with porous medium. Heat and mass transfer effects on unsteady magneto hydrodynamics free convection flow near a moving vertical plate embedded in a porous medium was presented by Das and Jana [5]. Olajuwon [6] examined convection heat and mass transfer in a hydromagnetic flow of a second grade fluid past a semi-infinite stretching sheet in the presence of thermal radiation and thermo diffusion. Soret and Dufour effects on mixed convection in a non-Darcy porous medium saturated with micropolar fluid was studied by Srinivascharya [7]. Rebhi [8] studied unsteady natural convection heat and mass transfer of micropolar fluid over a vertical surface with constant heat flux. The governing equations were solved numerically using McCormack's technique and effects of various parameters were investigated on the flow. Sunil et al [9] studied the effect of rotation on a layer of micropolar ferromagnetic fluid heated from below saturating a porous medium. The resulted non-linear coupled differential equations from the transformation were solved using finite-difference method. Reena and Rana [10] investigated double-diffusive convection in a micropolar fluid layer heated and cooled from below saturating a porous medium. A linear stability analysis theory and normal mode analysis method was used. Seddek [11] studied the effects of chemical reaction, thermophoresis and variable viscosity on steady hydromagnetic flow with heat and mass transfer over a flat plate in the presence of heat generation/absorption. Patil and Kulkarni [12] studied the effects of chemical reaction flow of a polar fluid through porous medium in the presence of internal heat generation. Double-diffusive convection radiation interaction on unsteady MHD flow over a vertical moving porous plate with heat generation and Soret effects was studied by Mohamed [13]. Chaudhary and Abhay [14] studied the effect of chemical reactions on MHD micropolar fluid flow past a vertical plate in slip-flow regime.

Modather et al. [15] studied MHD heat and mass transfer flow of a micropolar fluid over a vertical permeable plate in a porous medium without considering the effects of thermal-diffusion and heat generation. Motivated by these applications and previous work done, we studied the effects of thermal diffusion and heat generation on unsteady free convection heat and mass transfer flow of a micropolar fluid past a vertical permeable plate. The governing equations are solved analytically using perturbation method and effects of various physical parameters are discussed.

2.0 Mathematical Formulation

We consider unsteady, laminar non-Darcian mixed convection flow of a viscous, incompressible, electrically conducting micropolar fluid over an infinite vertical porous moving permeable plate in a saturated porous medium. A magnetic field of strength B_0 is applied perpendicular to the surface and the effect of the induced magnetic field is neglected. The x^* -axis is taken along the planar surface in the upward direction and the y^* -axis taken to be normal to it as shown in Fig. 1. Due to the infinite plane surface assumption, the flow variables are function of y^* and the t^* only. Initially, the fluid as well as the plate is at rest, but for time $t > 0$ the whole system is allowed to move with a constant velocity. At $t = 0$, the plate temperature is suddenly raised to T_w .

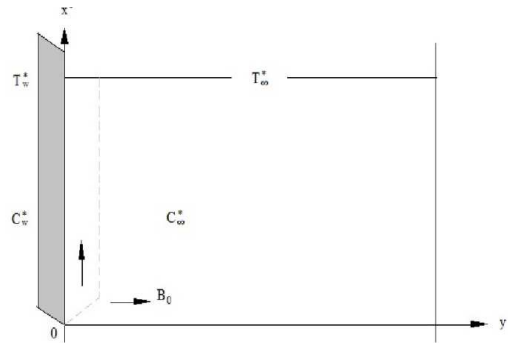


Fig1: Physical model.

The governing equations for such a motion are given by

$$\frac{\partial v^*}{\partial y^*} = 0 \tag{1}$$

$$\frac{\partial u^*}{\partial t^*} + v^* \frac{\partial u^*}{\partial y^*} = (v + v_r) \frac{\partial^2 u^*}{\partial y^{*2}} + 2v_r \frac{\partial w^*}{\partial y^*} + g\beta_T(T - T_\infty) + g\beta_c(C - C_\infty) - \sigma \frac{B_0^2 u^*}{\rho} - \frac{v+v_r}{K} u^* \tag{2}$$

$$\rho J^* \left(\frac{\partial w^*}{\partial t^*} + v^* \frac{\partial w^*}{\partial y^*} \right) = \gamma \frac{\partial^2 w^*}{\partial y^{*2}} \tag{3}$$

$$\frac{\partial T}{\partial t^*} + v^* \frac{\partial T}{\partial y^*} = \alpha \frac{\partial^2 T}{\partial y^{*2}} + \frac{Q_0(T - T_\infty)}{\rho C_p} \tag{4}$$

$$\frac{\partial C}{\partial t^*} + v^* \frac{\partial C}{\partial y^*} = D \frac{\partial^2 C}{\partial y^{*2}} + \frac{DK_t \partial^2 T}{T_m \partial y^{*2}} \tag{5}$$

Where (u^*, v^*) are the components of velocity at any point (x^*, y^*) , w^* is the component of the angular velocity normal to x^*, y^* plane, T is the temperature of the fluid and C is the mass concentration of the species in the flow. $\rho, v, v_r, g, \beta_T, \beta_c, \sigma, K, J^*, \gamma, \alpha, D, K_t, Q_0, T_m$ and C_p are the density, kinematic viscosity, kinematic rotational viscosity, acceleration due to gravity, coefficient of volumetric thermal expansion of the fluid, coefficient of volumetric mass expansion of the fluid, electrical conductivity of the fluid, permeability of the medium, microinertia per unit mass, spin gradient viscosity, thermal diffusivity, molecular diffusivity thermal diffusion ratio, constant heat flux per unit, mean fluid temperature and specific heat at constant pressure respectively.

The appropriate boundary conditions for the problem are

$$\begin{aligned} u^* = u_p^*, w^* = -n_1 \frac{\partial u^*}{\partial y^*}, T = T_\infty + \varepsilon(T_w - T_\infty)e^{n^* t^*} \\ C = C_\infty + \varepsilon(C_w - C_\infty)e^{n^* t^*} \text{ as } y^* = 0 \\ u^* \rightarrow 0, w^* \rightarrow 0, T \rightarrow T_\infty, C \rightarrow C_\infty \text{ as } y^* \rightarrow \infty \end{aligned} \tag{6}$$

The following comments should be made about the boundary condition used for the microrotation term; When $n_1=0$, $w^*=0$. This represents the case of concentrated particle flows in which the microelements close to the wall are unable to rotate [16]. The case corresponding to $n_1=0.5$ results in the vanishing of the antisymmetric part of the stress tensor and represent weak concentration. The case corresponding to $n_1=1$ is representative of turbulent boundary layer flows[17]. Thus, for $n_1=0$, the particle are not free to rotate near the surface. However, as $n_1=0.5$ and 1, the microrotation term gets augmented and induces flow enhancement.

Integrating equation (1), we get

$$v^* = -V_0 \tag{7}$$

Where V_0 is a scale of suction velocity, which has a non-zero positive constant.

Let us introduce the following dimensionless variables:

$$\begin{aligned} u = \frac{u^*}{U_0}, v = \frac{v^*}{V_0}, y = \frac{V_0 y^*}{\nu}, U_p = \frac{u_p^*}{U_0}, w = \frac{\nu}{U_0 V_0} w^*, t = \frac{t^* V_0^2}{\nu} \\ \theta = \frac{T - T_\infty}{T_w - T_\infty}, \phi = \frac{C - C_\infty}{C_w - C_\infty}, n = \frac{n^* \nu}{V_0^2}, J = \frac{V_0^2 J^*}{\nu^2} \end{aligned} \tag{8}$$

Substituting equation (8) into equations (2) – (5) yield the following dimensionless equations:

$$\frac{\partial u}{\partial t} - \frac{\partial u}{\partial y} = (1 + \beta) \frac{\partial^2 u}{\partial y^2} + 2\beta \frac{\partial w}{\partial y} + Gr\theta + Gc\phi - Mu - \frac{1+\beta}{K'} u \tag{9}$$

$$\frac{\partial w}{\partial t} - \frac{\partial w}{\partial y} = \frac{1}{\eta} \frac{\partial^2 w}{\partial y^2} \tag{10}$$

$$\frac{\partial \theta}{\partial t} - \frac{\partial \theta}{\partial y} = \frac{1}{Pr} \frac{\partial^2 \theta}{\partial y^2} + H\theta \tag{11}$$

$$\frac{\partial \phi}{\partial t} - \frac{\partial \phi}{\partial y} = \frac{1}{Sc} \frac{\partial^2 \phi}{\partial y^2} + Sr \frac{\partial^2 \theta}{\partial y^2} \tag{12}$$

Where $\eta = \frac{\mu J^*}{\gamma} = \frac{2}{2+\beta}$

And $M = \frac{\sigma B_0^2 \nu}{\rho \nu_0^2}$ the magnetic field parameter, $Gr = \frac{\nu \beta_T g (T_w - T_\infty)}{U_0 \nu_0^2}$ the Grashof number,
 $Gc = \frac{\nu \beta_c g (C_w - C_\infty)}{\nu_0^2 U_0}$ the modified Grashof number, $Pr = \frac{\nu}{\alpha} = \frac{\nu \rho C_p}{K}$ the Prandth number,
 $Sc = \frac{\nu}{D}$ the Schmidt number, $H = \frac{\nu Q_0}{\rho C_p \nu_0^2}$ the heat source parameter, $K' = \frac{K U_0 \nu_0^2}{\nu^2}$ permeability parameter,
 $Sr = \frac{DK_t (T_w - T_\infty)}{T_m \nu (C_w - C_\infty)}$ and $\beta = \frac{\nu_r}{\nu}$ the dimensionless viscosity ratio.
 The corresponding boundary conditions are

$$u = U_p, \theta = 1 + \varepsilon e^{nt}, w = -n_1 \frac{\partial u}{\partial y}, \phi = 1 + \varepsilon e^{nt} \text{ at } y = 0$$

$$u \rightarrow 0, w \rightarrow 0, \theta \rightarrow 0, \phi \rightarrow 0 \text{ as } y \rightarrow \infty \tag{13}$$

3.0 Method of Solution

To find the analytical solution of the above system of partial differential equations (9) – (12) subject to the boundary conditions (13), we assume a perturbation of the form:

$$u = u_0(y) + \varepsilon e^{nt} u_1(y) + o(\varepsilon^2) \tag{14}$$

$$w = w_0(y) + \varepsilon e^{nt} w_1(y) + o(\varepsilon^2) \tag{15}$$

$$\theta = \theta_0(y) + \varepsilon e^{nt} \theta_1(y) + o(\varepsilon^2) \tag{16}$$

$$\phi = \phi_0(y) + \varepsilon e^{nt} \phi_1(y) + o(\varepsilon^2) \tag{17}$$

Substituting equations (14) – (17) into equations (9) - (12), neglecting the higher order terms of $O(\varepsilon^2)$ to obtain the following set of equations:

$$(1 + \beta)u_0'' + u_0' - C_1 u_0 = -Gr\theta_0 - Gc\phi_0 - 2\beta w_0' \tag{18}$$

$$(1 + \beta)u_1'' + u_1' - C_2 u_1 = -Gr\theta_1 - Grc\phi_1 - 2\beta w_1' \tag{19}$$

$$w_0'' + \eta w_0' = 0 \tag{20}$$

$$w_1'' + \eta w_1' - \eta n w_1 = 0 \tag{21}$$

$$\theta_0'' + Pr\theta_0' + PrH\theta_0 = 0 \tag{22}$$

$$\theta_1'' + Pr\theta_1' + Pr(H - n)\theta_1 = 0 \tag{23}$$

$$\phi_0'' + Sc\phi_0' + SrSc\theta_0'' = 0 \tag{24}$$

$$\phi_1'' + Sc\phi_1' - Scn\phi_1 + ScSr\theta_1'' = 0 \tag{25}$$

Where $C_1 = M + \frac{1+\beta}{K'}$, $C_2 = n + M + \frac{1+\beta}{K'}$

The corresponding boundary conditions can be written as

$$\left\{ \begin{aligned} u_0 = U_p, u_1 = 0, w_0 = -n_1 u_0', w_1 = -n_1 u_1' \\ \theta_0 = 1, \theta_1 = 1, \phi_0 = 1, \phi_1 = 1 \\ u_0 = 0, u_1 = 0, w_0 = 0, w_1 = 0, \theta_0 = 0, \theta_1 = 0, \phi_0 = 0, \phi_1 = 0 \text{ at } y \rightarrow \infty \end{aligned} \right. \tag{26}$$

The solution of (18) - (25) satisfying the boundary conditions (26) are given by

$$u = A_1 e^{-m_2 y} + A_2 e^{-m_1 y} + A_3 e^{-Scy} + A_4 e^{-\eta y} + (A_5 e^{-m_6 y} + A_6 e^{-m_3 y} + A_7 e^{-m_4 y} + A_8 e^{-m_5 y}) \varepsilon e^{nt} \tag{27}$$

$$w = B_1 e^{-\eta y} + \varepsilon e^{nt} B_2 e^{-m_5 y} \tag{28}$$

$$\theta = e^{-m_1 y} + \varepsilon e^{nt} e^{-m_3 y} \tag{29}$$

$$\phi = E_1 e^{-Scy} + E_2 e^{-m_1 y} + \varepsilon e^{nt} (E_3 e^{-m_6 y} + E_4 e^{-m_3 y}) \tag{30}$$

Where

$$m_1 = \frac{Pr + \sqrt{Pr^2 - 4PrH}}{2}, m_2 = \frac{1 + \sqrt{1 + 4(1 + \beta)C_1}}{2(1 + \beta)}, m_3 = \frac{Pr + \sqrt{Pr^2 - 4Pr(H - n)}}{2}, m_4 = \frac{Sc + \sqrt{Sc^2 + 4Scn}}{2}, m_5 = \frac{\eta + \sqrt{\eta^2 + 4\eta n}}{2},$$

$$m_6 = \frac{1 + \sqrt{1 + 4(1 + \beta)C_2}}{2(1 + \beta)}, E_2 = \frac{-ScSr}{m_1^2 - Scm_1}, E_1 = 1 - E_2, A_2 = \frac{-(Gr + GcE_2)}{(1 + \beta)m_1^2 - m_1 - C_1},$$

$$A_3 = \frac{-GcE_1}{(1 + \beta)Sc^2 - Sc - C_1}, A_4 = \frac{2\beta\eta n_1(m_2 U_p - m_2 A_2 - m_2 A_3 + m_1 A_2 + ScA_3)}{((1 + \beta)\eta^2 - \eta - C_1) + 2\beta\eta n_1(m_2 - \eta)}, A_1 = U_p - A_2 - A_3 - A_4$$

$$B_1 = n_1(m_2 A_1 + m_1 A_2 + ScA_3 + \eta A_4), E_4 = \frac{-SrScm_3^2}{m_3^2 - Scm_3 - Scn}, E_3 = 1 - E_4, A_6 = \frac{-(Gr + GcE_4)}{(1 + \beta)m_3^2 - m_3 - C_2}, A_7 = \frac{-GcE_3}{(1 + \beta)m_4^2 - m_4 - C_2}, A_8 = \frac{2\beta m_5 n_1(m_3 A_6 + m_4 A_7 - m_6 A_6 - m_6 A_7)}{((1 + \beta)m_5^2 - m_5 - C_2) + 2\beta m_5 n_1(m_6 - m_5)}$$

$$A_5 = -(A_6 + A_7 + A_8), B_2 = n_1(m_6 A_5 + m_3 A_6 + m_4 A_7 + m_5 A_8)$$

The local skin friction coefficient, couple stress coefficient, Nusselt number and Sherwood number are important physical quantities of engineering interest. The wall shear stress may be written as

$$\tau_w^* = \rho U_0 \nu_0 [1 + (1 - n_1)\beta] u'(0) \tag{31}$$

and the skin friction coefficient(Cf) at the wall is given by

$$Cf = \frac{2\tau_w}{\rho U_0 \nu_0} = 2[1 + (1 - n_1)\beta] u'(0) = -2[1 + (1 - n_1)\beta][m_2 A_1 + m_1 A_2 + ScA_3 + \eta A_4 + \varepsilon e^{nt}(m_6 A_5 + m_3 A_6 + m_4 A_7 + m_5 A_8)] \tag{32}$$

The couple stress coefficient (C'_w) at the plate is written as

$$C'_w = \frac{M_w v^2}{y u_0 v_0^2} = w'(0) \text{ where } M_w \text{ is the wall couple stress.}$$

$$= -(\eta B_1 + \varepsilon e^{nt} B_2 m_5) \tag{33}$$

The rate of heat transfer at the surface in terms of the Nusselt number is given by

$$Nu = \frac{x \left(\frac{\partial T}{\partial y} \right)}{(T_\infty - T_w)}$$

$$Nu Re_x^{-1} = -\theta'(0) = m_1 + \varepsilon e^{nt} m_3 \tag{34}$$

Where $Re_x = \frac{x v_0}{\nu}$

The rate of mass transfer at the surface in terms of the local Sherwood number is given by

$$Sh = \frac{\left(\frac{\partial c}{\partial y^*} \right)_{y^*=0}}{C_\infty - C_w}$$

$$Sh Re_x^{-1} = -\phi'(0) = Sc E_1 + m_1 E_2 + \varepsilon e^{nt} (m_4 E_3 + m_3 E_4) \tag{35}$$

4.0 Results and Discussion

Numerical evaluation of the analytical solutions reported in the previous section was performed. The numerical calculations for the distribution of translational velocity, microrotational velocity, temperature and concentration across the boundary layer for various values of the parameter including skin-friction coefficient, couple stress coefficient, Nusselt number and Sherwood number was carried out and the results are presented in graphical and tabular form. This was done to illustrate the influence of the various parameter involved. In this study, we have chosen $\varepsilon=0.01$, $n=0.1$, $\beta=1$ and $Up=0.5$ while Sr , t , Sc , H , Pr , Gc , Gr , n_1 , K' and M are varied over a range.

4.1 Effect of Parameters on Translational Velocity Profiles

The effect parameters on velocity profiles are shown in Fig.2 – Fig.10. Fig.2 illustrates the variation of translational velocity distribution across the boundary layer for various values of the Soret number Sr . The figure shows that the translational velocity of the fluid flow increases with increase in the Soret parameter Sr across the boundary layer and is maximum near at distant($y=1$). Thus the effect of increasing values of the Soret parameter Sr is to increase the momentum boundary layer thickness. Fig.3 shows that increase in heat source parameter increases the translational velocity profiles. The effect of magnetic field parameter on translational velocity distribution profiles across the boundary layer is indicated presented in Fig.4. It is obvious that the effect of increasing values of the magnetic field parameter M results in a decreasing translational velocity distribution across the boundary layer. This is due to the fact that the introduction of transverse magnetic field normal to the flow direction has a tendency to create a drag force due to Lorentz force and hence results in retarding the velocity profiles. Fig.5 depict the effect of permeability parameter(K') on translational velocity distribution profiles and it is obvious that as permeability parameter(K') increases, the velocity increases along the boundary layer thickness. Fig.6 shows the effect of the parameter n_1 , which relates to the microgyration vector and the shear stress on the translational velocity distribution profiles. It is observed that velocity increases with increasing values of the parameter n_1 . Fig.7 and Fig.8 illustrates the translational velocity profiles for different values of Grashof number (Gr) and modified Grashof number (Gc) respectively. It can be seen that an increase in Gr or Gc leads to a rise in velocity profiles. Fig.9 present the translational velocity distribution profile for different values of the Prandtl number(Pr). The results show that the effect of increasing values of Pr result in a decrease in the velocity. For different values of the Schmidt number Sc , fig.10 shows that the effect of increasing values of Sc results in a decreasing translational velocity distribution

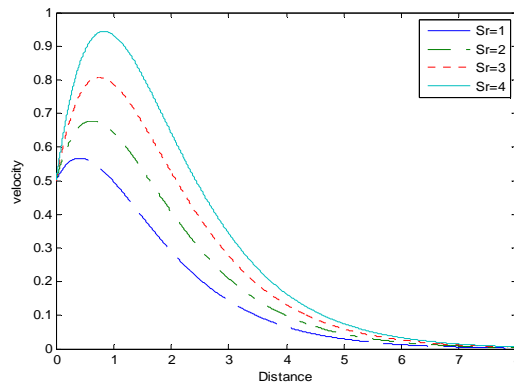


Fig 2: Velocity distribution profiles for different values of Soret number

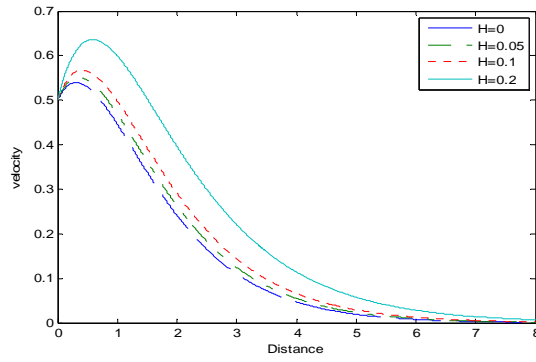


Fig.3: Velocity distribution profiles for different values of heat source parameter

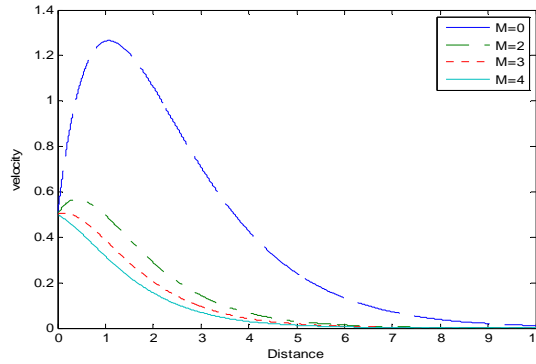


Fig.4: Velocity distribution profiles for different values of magnetic field parameter.

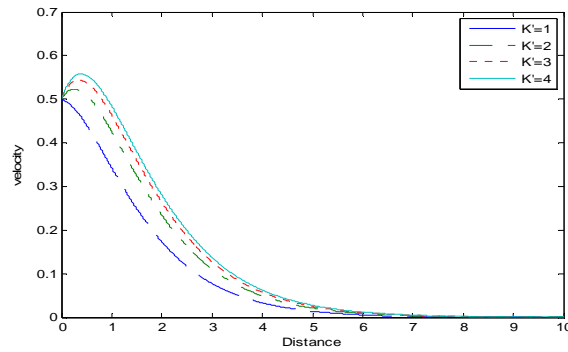


Fig.5: Velocity distribution profiles for different values of permeability parameter.

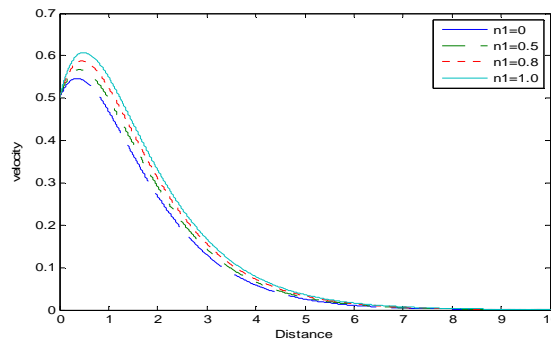


Fig.6: Velocity distribution profiles for different values of parameter related to micro gyration vector and shear stress

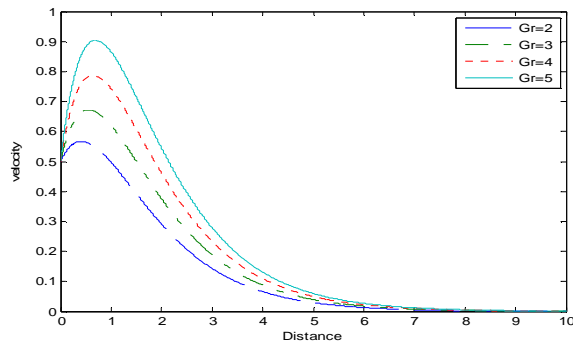


Fig.7: Velocity distribution profiles for different values of Grashof number

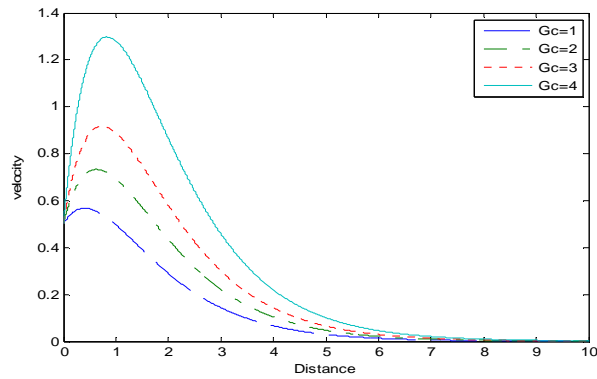


Fig.8: velocity distribution profiles for different values of modified Grashof number.

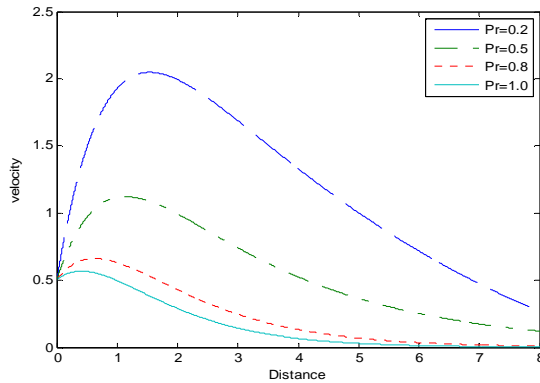


Fig.9: Velocity distribution profiles for different values of Prandtl number.

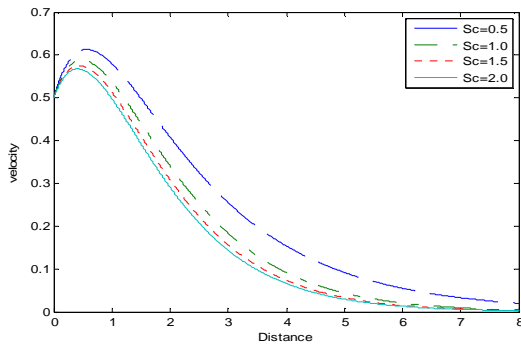


Fig.10: Velocity distribution profiles for different values of Schmidt number.

4.2 Effect of Parameters on Microrotational Velocity Profiles

Fig.11 displays that microrotational velocity decreases as Sr increases across the boundary layer. Fig.12 shows that the effect of increasing heat source parameter is to decrease the microrotational velocity. Fig.13 depict the microrotational velocity profiles for different values of the magnetic field parameter (M). In contrast to translational velocity distribution profiles, the microrotational velocity distribution increases with increase in the magnetic field parameter. The effects due to permeability parameter (K') on microrotational velocity are shown in Fig.14. It is observed that as permeability parameter increases, the microrotational velocity decreases Fig.15 show the effect of the parameter n_1 , which relates to the microgyration vector and the shear stress on microrotation profiles. It is observed that the microrotational decreases for increasing values of n_1 . Fig.16 and Fig.17 elucidate that the effect of increasing G_c or G_r is to decrease microrotational velocity. Fig.18 shows that as Prandtl number increase, microrotational velocity increases. Fig.19 shows that the microrotational velocity increases as SC increases

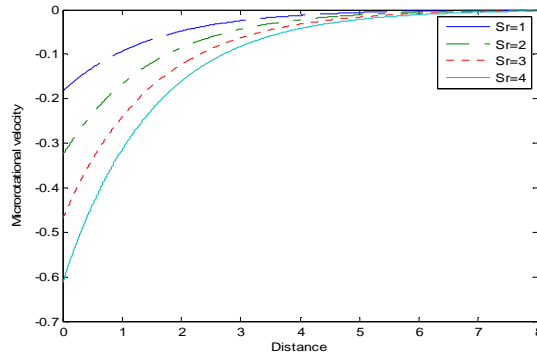


Fig.11: Microrotational velocity distribution profiles for different values of Soret number

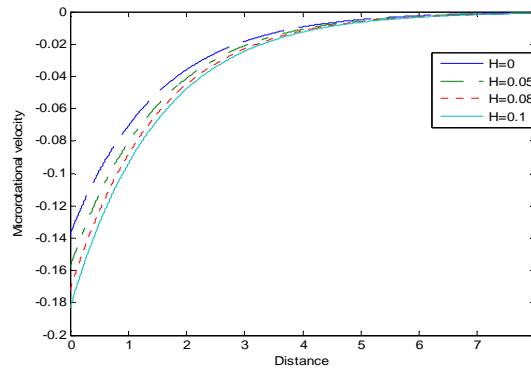


Fig.12: Microrotational velocity distribution for different values of heat source parameter.

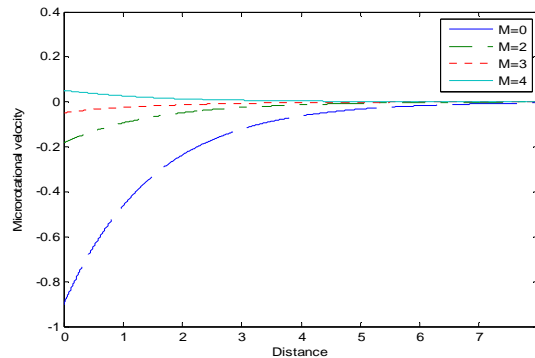


Fig.13: Microrotational velocity for different values of magnetic field parameter.

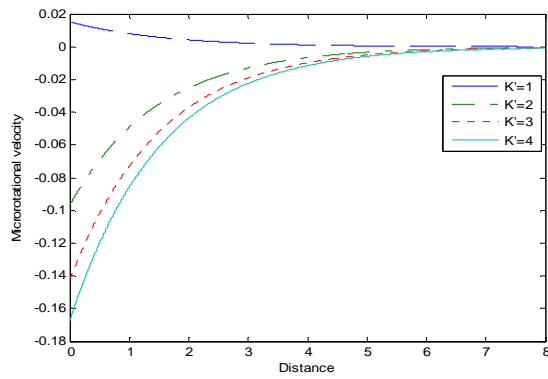


Fig.14: Microrotational velocity distribution for different values of permeability parameter.

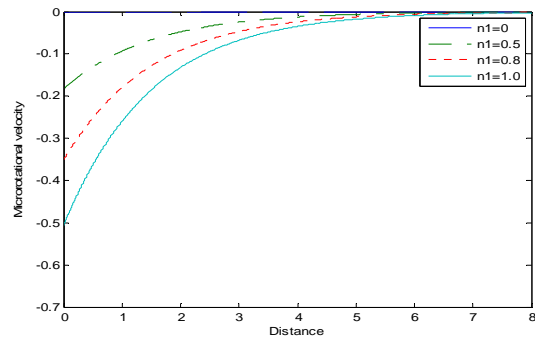


Fig.15: Microrotational velocity distribution for different values of parameter related to microgyration vector and shear stress.

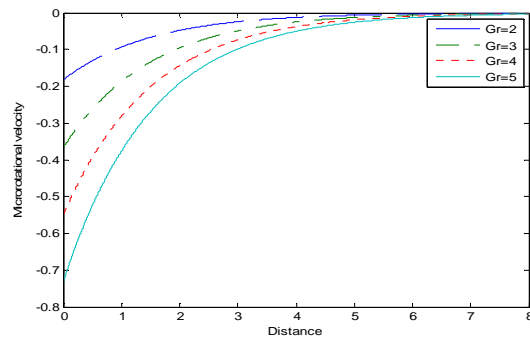


Fig.16: Microrotational velocity distribution profiles for different values of Grashof number.

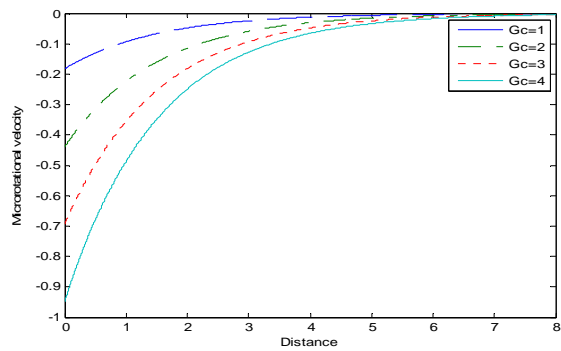


Fig.17: Microrotational velocity distribution profiles for different values of modified Grashof number.

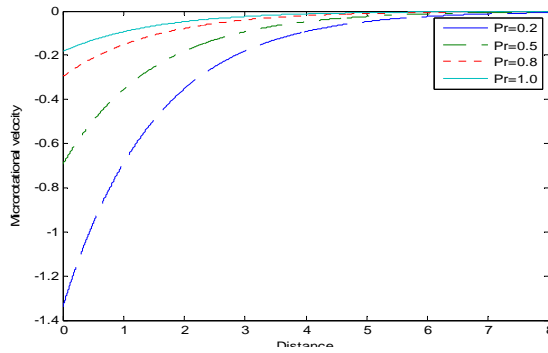


Fig.18: Microrotational velocity distribution profiles for different values of Prandtl number.

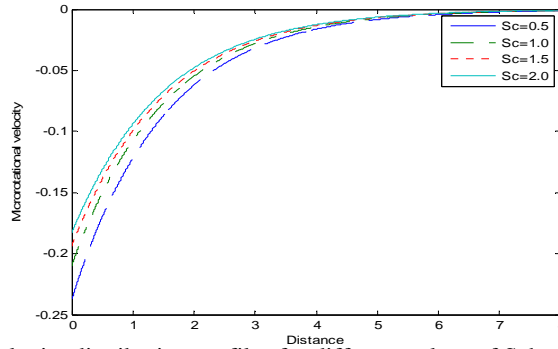


Fig. 19: Microrotational velocity distribution profiles for different values of Schmidt number.

4.3 Effects of Parameters on Temperature Profiles

Fig.21 presents the effect of the Prandtl number Pr on the temperature profiles. Increasing the values of Pr has the tendency to decrease the fluid temperature in the boundary layer as well as the thermal boundary-layer thickness. This causes the wall slope of the temperature to decrease as Pr increasing causing the Nusselt number to increase as can be clearly seen in Table3.

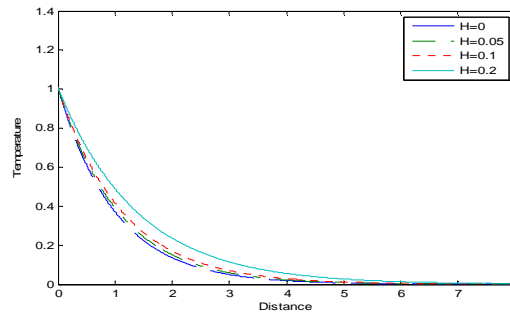


Fig. 20: Temperature distribution profiles for different values of heat source parameter.

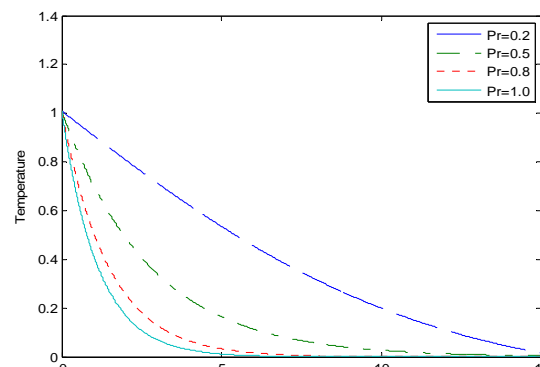


Fig.21: Temperature distribution profiles different values of Prandtl number.

4.4 Effects of Parameters on Concentration Profiles

Fig.22 shows the variation of concentration distribution across the boundary layer for different values of Soret number. It is observed from this figure that the concentration of the fluid increases with increase in the Soret parameter Sr . Fig.23 shows that the effects of increasing heat source parameter is to increase the concentration of the fluid. Fig.24 indicates that the effect of increasing Prandtl number is to decrease the concentration of the fluid. .

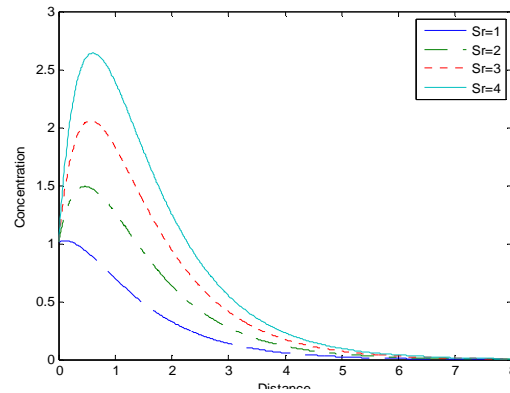


Fig. 22: Concentration distribution profiles for different values of Soret number.

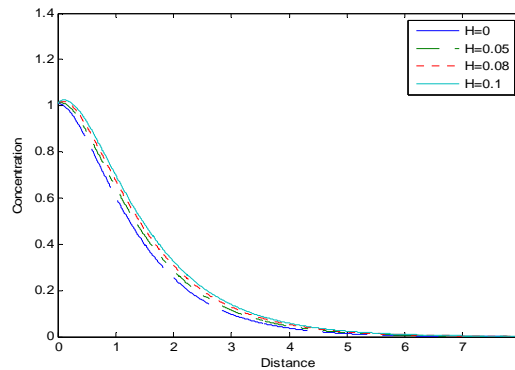


Fig. 23: Concentration distribution profiles for different values of heat source parameter.

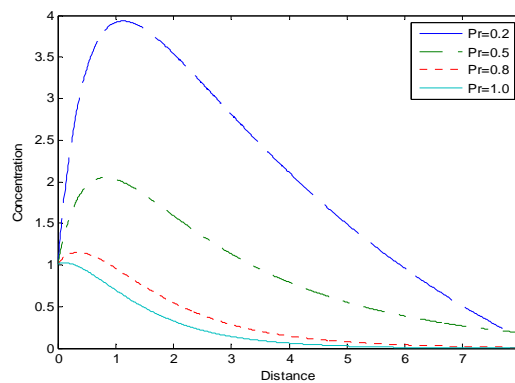


Fig. 24: Concentration distribution profiles for different values of Prandtl number.

4.5 Effects of Parameters on Skin Friction Coefficient, Couple Stress Coefficient, Nuselt Number and Sherwood Number.

Table1 shows the effect of Sr , Up , Sc , K' and H on the skin friction coefficient C_f . It is observed from the table that Sr , K' and H increases the skin friction coefficient while Up and Sc decreases the skin friction coefficient. Table2 also shows that Sr , K' and H increases the couple stress coefficient while Up and Sc decreases the couple stress coefficient. Table3 display the effect of Pr and H on the Nusselt number. It is clear from the tablethat increase in Prandtl number increases the rate of heat transfer while increase in heat source parameter decreases the rate of mass transfer. Table4 indicate effect of Sr , H , Sc and Pr on Sherwood number. As it can be seen from the table, Sr , H and Pr increase rate of

mass transfer. Table5 illustrate the variation of the coefficients of skin friction, couple stress coefficient, heat transfer and mass transfer with various value of t. It can be seen that skin friction coefficient, couple stress coefficient, heattransfer and mass transfer increase with time. These results are in excellent agreement with the results of Chaudhary and Abhay[14] , Modather et al[15] and Das[5]

Table 1: Effect of Sr, Up, H, Sc and K' parameter on C_f with $E=0.01$, $n=0.1$, $n_1=0.5$, $\beta=1$, $Gr=2$, $Gc=1$, $M=2$, $Pr=1$, $t=1$,

Sr	Up	Sc	K'	H	C_f
0.5	0.5	2.0	5.0	0.1	0.6706
1.0	0.5	2.0	5.0	0.1	0.1004
2.0	0.5	2.0	5.0	0.1	1.9600
1.0	0	2.0	5.0	0.1	3.7298
1.0	0.5	2.0	5.0	0.1	1.1004
1.0	1.0	2.0	5.0	0.1	-1.5291
1.0	0.5	0.5	5.0	0.1	1.4250
1.0	0.5	1.0	5.0	0.1	1.2591
1.0	0.5	1.5	5.0	0.1	1.1630
1.0	0.5	2.0	1.0	0.1	-0.0916
1.0	0.5	2.0	2.0	0.1	0.5796
1.0	0.5	2.0	3.0	0.1	0.8543
1.0	0.5	2.0	5.0	0.05	0.9482
1.0	0.5	2.0	5.0	0.08	1.0348
1.0	0.5	2.0	5.0	0.1	1.1004

Table 2: Effect of Sr, Up, H, Sc and K' parameter on C'_w with $E=0.01$, $n=0.1$, $n_1=0.5$, $\beta=1$, $Gr=2$, $Gc=1$, $M=2$, $Pr=1$, $t=1$,

Sr	Up	Sc	K'	H	C'_w
0.5	0.5	2.0	5.0	0.1	0.0750
1.0	0.5	2.0	5.0	0.1	0.1228
2.0	0.5	2.0	5.0	0.1	0.2184
1.0	0	2.0	5.0	0.1	0.4150
1.0	0.5	2.0	5.0	0.1	0.1228
1.0	1.0	2.0	5.0	0.1	-0.1694
1.0	0.5	0.5	5.0	0.1	0.1589
1.0	0.5	1.0	5.0	0.1	0.1405
1.0	0.5	1.5	5.0	0.1	0.1298
1.0	0.5	2.0	1.0	0.1	-0.0097
1.0	0.5	2.0	2.0	0.1	0.0649
1.0	0.5	2.0	3.0	0.1	0.0954
1.0	0.5	2.0	5.0	0.05	0.1059
1.0	0.5	2.0	5.0	0.08	0.1155
1.0	0.5	2.0	5.0	0.1	0.1228

Table3:Effect of Pr and H parameter on $NuRe_x^{-1}$ with $n=0.1$, $n_1=0.5$, $\beta=1$, $Gr=2$, $Gc=1$, $M=2$, $Pr=1$, $Up=0.5$, $Sr=1$, $t=1$

Pr	H	$NuRe_x^{-1}$
0.5	0.1	0.3673
0.8	0.1	0.6917
1.0	0.1	0.8984
1.0	0.05	0.9588
1.0	0.08	0.9236
1.0	0.1	0.8984

Table 4: Effect of Sr, H, Sc and Pr, parameter on $ShRe_x^{-1}$ with $n=0.1$, $E=0.01$, $n_1=0.5$, $\beta=1$, $Gr=2$, $Gc=1$, $M=2$, $Up=0.5$, $t=1$

Sr	H	Sc	Pr	$ShRe_x^{-1}$
0.5	0.1	2.0	1.0	0.8861
1.0	0.1	2.0	1.0	-0.2511
2.0	0.1	2.0	1.0	-2.5253
1.0	0.05	2.0	1.0	-0.1095
1.0	0.08	2.0	1.0	-0.1897
1.0	0.1	2.0	1.0	-0.2511
1.0	0.1	0.5	1.0	-0.0621
1.0	0.1	1.0	1.0	-0.1251
1.0	0.1	1.5	1.0	-0.1881
1.0	0.1	2.0	0.5	-3.5140
1.0	0.1	2.0	0.8	-0.9216
1.0	0.1	2.0	1.0	-0.2511

Table 5: Unsteady behavior of the coefficient of skin-friction, couple stress coefficient, heat transfer and mass transfer with various value of t when $E=0.01$, $n=0.1$, $n_1=0.5$, $\beta=1$, $Gr=2$, $Gc=1$, $M=2$, $Pr=1$, $Sr=1$, $H=0.1$, $Sc=2$, $K'=5$ and $Up=0.5$.

T	C_f	C^*w	$NuRe_x^{-1}$	$ShRe_x^{-1}$
0	1.096	0.1224	0.8973	-0.2513
1	1.1004	0.1228	0.8984	-0.2511
3	1.1085	0.1238	0.9008	-0.2504
5	1.1185	0.1251	0.9038	-0.2496
10	1.1541	0.1296	0.9145	-0.2467
20	1.3095	0.1491	0.9612	-0.2341
30	1.7321	0.2023	1.0882	-0.1999

5.0 Conclusion

An analytical study of the MHD heat and mass transfer of the laminar flow of an incompressible, electrically conducting micropolar fluid over an infinite vertical moving plate in a saturated porous medium was conducted. The resulting partial differential equations which describe the problem, are transformed to dimensionless equations using dimensionless variables. Then solve the equations analytically by using perturbation technique. The results are discussed through graphs and tables for different values of parameters entering into the problem. Following conclusions can be drawn from the results obtain:

- * Increase in Soret number and heat source parameter, increases the translational velocity and concentration of the fluid while it decreases the microrotational velocity.
- * Increase in heat source parameter increases the temperature of the fluid
- * Increase in Sr and H decreases the rate of mass transfer.
- * In the presence of a uniform magnetic field, increase in the strength of the applied magnetic field decelerated the fluid motion along the wall of the plate inside the boundary layer, whereas the microrotational velocity of the fluid along the wall of the plate increased.
- * Increase Sr and H increases the skin friction coefficient and couple stress coefficient and decreases the rate of mass transfer.

References

- [1]. Erigen A.C, Theory of micropolar fluids *J. math.mech.* ,1966,16, pp.1-18.
- [2]. Raju M.C, Verna S.K.,Reddy P.V and Saha .S Soret effects due to natural convection between heated inclined plates with magnetic field. *Journal of mechanical engineering*, 39,2008 pp. 65-70,
- [3]. Aurangzaib, S.S, Effects of Soret and Dufour on unsteady MHD flow by mixed convection over a vertical surface in porous media with internal heat generation, chemical reaction and hall current. *Canadian journal on science and engineering mathematics*, Vol.2,2011, N0.4,
- [4] Kumar. R. and Singh K. D Mathematical modeling of Soret and hall effects on oscillatory MHD free convective flow of radiating fluid in a rotating vertical porous channel filled with porous medium. *Int. J. App. Math and mech.*, 8(6):2012, 49-68.

- [5]. Das K, Jana S. Heat and mass transfer effects on unsteady MHD free convection flow near a moving vertical plate in a porous medium. *Bull. Soc. Banja Luka*, 2010, 17:15-32.
- [6]. Olajuwon. B.I. Convection heat and mass transfer in a hydromagnetic flow of a second grade fluid in the presence of thermal radiation and thermal diffusion. *Int. commu. Heat and mass*, 2011, 38:377-382.
- [7]. Srinivasacharya.D., Ramreddy. Ch., Soret and Dufour effect on mixed convection in a non-Darcy porous medium saturated with micropolar fluid, *Non-analysis modelling and control*, vol.16, No.1, 2011, 100-115.
- [8]. Rehbi, A.D., Tariq, A.A. Benbella, A.S. Mahoud, A.A. Unsteady natural convection heat transfer of micropolar fluid over a vertical surface with constant Heat flux, *Turkish J. Eng. Env. Sci.*, Vol. 31, 2007, pp. 225-233
- [9]. Sunil, A. Sharma, A. Bharti, P.K. and Shandi, R.G. "Effect of rotation on a layer of micropolar ferromagnetic fluid heated from below saturating a porous medium, *International Journal of Engineering science*, vol. 44 no. 11-12, 2006, pp. 683-698.
- [10]. Reena I. and Rana U.S., Linear stability of thermo solutal convection in a micropolar fluid saturating a porous medium, *International Journal of Application and Applied mathematics*, vol. 4, no. 1, 2009. pp.62-87
- [11]. Seddek M.A. Finite-element method for effects of chemical reaction, variable viscosity, thermophoresis and heat generation/absorption on a boundary layer hydromagnetic flow with heat and mass transfer over a heat surface. *Acta mech.* 177, 2005, pp. 1-18.
- [12]. Patil, P.M. and Kulkarni P.S. Effects of chemical reaction on free convective flow of a polar fluid through a porous medium in the presence of internal heat generation, *Int. Therm. Sci.* , 4, 2008, Pp. 1043-1054.
- [13]. Mohamad. Double diffusive convection-radiation interaction on unsteady MHD flow over a vertical moving porous plate with heat generation and Soret effect, *Applied Mathematical sciences* , 13, 2009, pp. 629-651.
- [14]. Chaudhary, R.C. and Abhay K.J . Effect of chemical reaction on MHD micropolar fluid flow past a vertical plate in slip-flow regime. *Appl. Math. Mech. Engl. Ed.* 29(9):2008, 117-1194.
- [15]. Modather M, Rashad A.M, Chamkha A.J. Study of MHD heat and mass transfer oscillatory flow of a micropolar fluid over a vertical permeable plate in a porous medium. *Turkis J.Zeng. Env. Sci.*, vol33, 2009, 245-257.
- [16]. Jena, S.K and Mathur, M.N., Free convection in the laminar boundary layer flow of a thermomicropolar fluid past a vertical flat with suction/injection, *Acta Mechanica*, 42, 1982, 227..
- [17]. Peddieson, J., Boundary layer theory for a micropolar fluid, *Int. J. Eng. Sci.*, 10, 1972, 23-29